Chemical and Biological Technologies in Agriculture

RESEARCH

Open Access

# Arbuscular mycorrhizal fungi regulate polyamine metabolism and antioxidant activity of *Sorghum halepense* grown in uranium-contaminated soils

Yun-Mu Zhang[1], Bin Liu[2], Yun-Mei Lu[1], Ren-Hua Huang[1*], Abeer Hashem[4], Elsayed Fathi Abd-Allah[5] and Qiang-Sheng Wu[3]

## Abstract

**Background** Uranium (U) contamination poses a serious threat to ecosystems. Phytoremediation offers an eco-friendly solution but is often limited by metal toxicity in plants. Arbuscular mycorrhizal fungi (AMF) can enhance plant tolerance and improve phytoremediation efficiency, while their specific interaction with polyamine (PA) metabolism under U stress remains unclear. This study investigates how AMF inoculation influences PA metabolism, antioxidant activity, and U uptake in *Sorghum halepense* (L.) Pers. ( *S. halepense*).

**Results** U stress disrupted PA metabolism in *S. halepense*, leading to significant accumulation of putrescine (Put), spermidine (Spd), and spermine (Spm), with Put showing the most pronounced increase. This metabolic disturbance was accompanied by elevated levels of hydrogen peroxide ($H_2O_2$) and malondialdehyde (MDA), ultimately resulting in oxidative damage. Inoculation with *Funneliformis mosseae* (*F. mosseae*) enhanced the activities of key metabolic enzymes—diamine oxidase, polyamine oxidase, arginine decarboxylase, and ornithine decarboxylase—thereby promoting the conversion of Put to Spd and Spm. This shift increased the (Spd + Spm)/Put ratio by 1.99-fold and restored PA homeostasis. Consequently, AMF inoculation reduced $H_2O_2$ and MDA levels, raised the oxygen radical absorbance capacity (ORAC) in roots by 1.30-fold, and enhanced U immobilization, elevating root U content by 1.99-fold compared with the non-inoculated control.

**Conclusions** *F. mosseae* mitigated U-induced oxidative stress in *S. halepense* through the modulation of PA metabolism, thereby enhancing antioxidant capacity and contributing to increased U immobilization in roots. Accordingly, *F. mosseae* emerges as a promising symbiotic strategy for the phytoremediation of U-contaminated soils.

**Keywords** Arbuscular mycorrhizal fungi, Phytoremediation, Polyamine, Uranium, *Sorghum halepense*

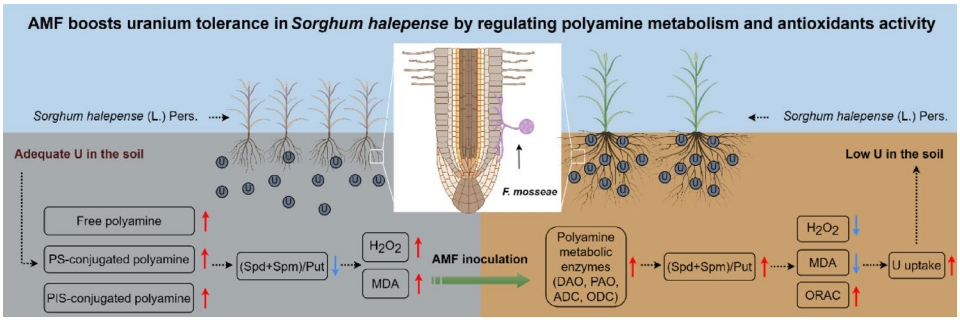
*Correspondence:
Ren-Hua Huang
hrh510@163.com

Full list of author information is available at the end of the article

© The Author(s) 2026. **Open Access** This article is licensed under a Creative Commons Attribution 4.0 International License, which permits use, sharing, adaptation, distribution and reproduction in any medium or format, as long as you give appropriate credit to the original author(s) and the source, provide a link to the Creative Commons licence, and indicate if changes were made. The images or other third party material in this article are included in the article's Creative Commons licence, unless indicated otherwise in a credit line to the material. If material is not included in the article's Creative Commons licence and your intended use is not permitted by statutory regulation or exceeds the permitted use, you will need to obtain permission directly from the copyright holder. To view a copy of this licence, visit http://creativecommons.org/licenses/by/4.0/.

Springer

**Graphical abstract**




## Introduction

Uranium (U), a heavy metal with combined chemical toxicity and radiological hazard, has become a significant environmental contaminant due to human activities such as mining and nuclear energy production, posing a persistent threat to ecosystems and human health [1, 2]. Phytoremediation is considered a promising, cost-effective, and environmentally friendly strategy for soil remediation [3]. However, the efficiency of remediating U-contaminated soil is constrained by two major bottlenecks: (i) U can induce excessive accumulation of reactive oxygen species (ROS) in plants, leading to severe oxidative damage [4], and (ii) U exhibits low bioavailability in soil, while plants generally have a limited capacity for its uptake and enrichment [5]. Consequently, developing synergistic strategies that simultaneously enhance plant antioxidant capacity and U absorption efficiency is crucial for improving the effectiveness of U phytoremediation.

Arbuscular mycorrhizal fungi (AMF) form symbiotic associations with the roots of over 80% of terrestrial plant species [6]. They significantly expand the root absorption area, improving host plant nutrition (particularly phosphorus and nitrogen) and water status, thereby comprehensively enhancing plant adaptability under abiotic stress [7]. In heavy metal-contaminated environments, AMF have been demonstrated to influence the migration and transformation of metals through direct hyphal uptake, cell wall binding, and sequestration [8]. These mechanisms can either immobilize metals in the root zone (phytostabilization) or, in some cases, promote plant metal uptake (phytoextraction) [9, 10]. *Funneliformis mosseae* (*F. mosseae*) is one of the most extensively studied and applied AMF species, with well-documented efficacy in promoting plant growth and enhancing tolerance to various heavy metals like zinc, cadmium (Cd), chromium (Cr), nickel (Ni), lead and arsenic (As) [11]. Some progress has also been made in the remediation of U-contaminated soil using AMF. Davies et al. employed multidisciplinary technical approaches—including radiotracer techniques, molecular biology, and imaging technologies—to elucidate the critical role of AMF in the uptake of radionuclides by plants [12]. Chen et al. demonstrated that inoculation with *Glomus intraradices* significantly increased U concentration in the roots of *Medicago truncatula* L. while improving plant growth [13]. Additionally, inoculation with *Glomus mosseae* and *Glomus intraradices* enhanced U enrichment in the roots of *Pteris vittata* L [14]. Ren et al. investigated the application of a triple symbiotic system involving the legume *Sesbania rostrata*, AMF, and rhizobia for the remediation of U-contaminated soil, demonstrating that the synergistic interaction significantly increased plant biomass and U uptake efficiency [15]. Dinsley et al. utilized advanced microscopic techniques to reveal how AMF alter the chemical speciation and subcellular distribution of U within plant roots, providing new insights into the mechanisms by which AMF enhanced plant-based remediation of U contamination [16].

Within the complex response network of plants to abiotic stresses such as heavy metals, polyamine (PA) metabolism plays a central role. In living organisms, PAs mainly exist in free, covalently conjugated or non-covalently conjugated forms [17]. The covalently conjugated-PAs can be divided into perchloric acid-soluble covalently conjugated PAs (PS-PAs) and perchloric acid-insoluble covalently conjugated PAs (PIS-PAs). Multiple PA forms engage in synergistic interactions, contributing to a comprehensive protective network that supports enhanced stress acclimation in plants. Putrescine (Put), spermidine (Spd), and spermine (Spm) are the most common PAs in higher plants. They are not only essential metabolites for basic cellular functions but also crucial stress-responsive signaling molecules [18–20]. PAs mitigate oxidative damage by directly scavenging ROS and stabilizing macromolecules and cellular membranes [21]. More importantly, PA metabolism constitutes a dynamic hub for redox signaling regulation. The activities of its biosynthetic enzymes (e.g., arginine decarboxylase, ADC; ornithine decarboxylase, ODC) and catabolic enzymes

(e.g., diamine oxidase, DAO; polyamine oxidase, PAO) are precisely modulated under stress [22]. This process facilitates the conversion of PA types (e.g., Put to Spd and Spm), and its catabolism is accompanied by the production of hydrogen peroxide ($H_2O_2$). This PA-derived $H_2O_2$ can act as a signaling molecule at low concentrations to activate the plant's systemic antioxidant defense system, whereas excessive accumulation exacerbates oxidative pressure [23]. Therefore, PA homeostasis, particularly the balance reflected by the ratio of higher protective PAs (Spd + Spm) to Put, is recognized as a sensitive indicator of plant stress tolerance [21]. Studies have shown that Spd and Spm accumulation is generally positively correlated with cold tolerance, and a high (Spd + Spm)/Put ratio serves as a key indicator of drought tolerance [24].

It is noteworthy that a functional convergence exists between AMF-enhanced plant stress resistance and PA-mediated stress response regulation. Research has established that the formation of the AMF symbiosis is initiated by a molecular dialogue involving root-exuded strigolactones and fungal-derived myc factors, which triggers extensive transcriptional and metabolic reprogramming in the host plant [25]. Evidence further indicates that under stresses such as drought and salinity, AMF can specifically modulate the host's PA metabolic profile [26, 27]. This suggests that AMF symbiosis likely interfaces with the host's intrinsic PA network—a key hub for redox signaling and stress adaptation. The modulation may operate through two interconnected mechanisms: on one hand, the improved phosphorus and nitrogen nutrition facilitated by AMF provides a foundational boost in substrates for PA biosynthesis [7]; On the other hand, more critically, AMF-induced physiological signals may engage in crosstalk with hydrogen peroxide signals generated from PA catabolism [28]. Such interaction at the signaling level could synergistically potentiate the host's antioxidant defense system, enhancing its resilience against stress. However, the tripartite interaction between U stress, AMF symbiosis, and PA metabolism remains entirely unexplored. Establishing this mechanistic link is essential to advance the fundamental understanding of mycorrhizal physiology in radionuclide-contaminated environments and to develop targeted bio-strategies for phytoremediation.

*Sorghum* genus has been recognized for its remarkable potential in phytoremediation of heavy metal-contaminated soils. *Sorghum* species exhibit several advantageous traits for this purpose, including high biomass production, efficient heavy metal accumulation and translocation, and robust tolerance to multiple abiotic stresses such as drought, salinity, and metal toxicity [29]. These characteristics are essential for effective phytoextraction, as high biomass directly correlates with the total amount of metals removed from the soil, while stress tolerance ensures plant survival and performance under challenging environmental conditions. Among sorghum species, *Sorghum halepense* (L.) Pers. (*S. halepense*) stands out as a particularly suitable candidate for phytoremediation. Importantly, unlike many other plants used in remediation that belong to edible leafy vegetables or cereal crops, *S. halepense* is a non-edible species, posing no risk of contaminating the food chain. This ecological safety feature, combined with its inherent remediation capacity and environmental adaptability, makes *S. halepense* an ideal choice for sustainable and safe phytoremediation practices.

To explore the potential of *F. mosseae* inoculation in enhancing the remediation capacity of *S. halepense* under U stress, this study comprehensively examined the contents of free and conjugated PAs and the activities of key metabolic enzymes in roots and leaves, assessed oxidative damage markers and total antioxidant capacity, and analyzed the accumulation and distribution of U within plant tissues. It aims to elucidate the novel mechanism through which AMF regulates PA metabolism to enhance plant U tolerance and influence U immobilization, thereby providing a theoretical basis for developing more effective AMF-assisted phytoremediation strategies for U-contaminated environments.

## Materials and methods

### Experimental design

A 2 × 2 factorial design was employed, combining two AMF inoculation treatments (non-inoculated vs. inoculated with *F. mosseae*) with two soil U levels: non-contaminated soil (NUCS, 0 mg/kg U) and U-contaminated soil (UCS, 44 mg/kg U). Each treatment replicates nine times.

### U-contaminated soil, plant growth conditions, mycoorhizal inoculation and plant sampling

The experimental soil was collected from the 0–20 cm surface layer of the garden at Southwest University of Science and Technology (31.481207° N, 104.728264° E). After removing weeds, the soil was homogenized, air-dried, and sieved through a 2 mm mesh, then mixed with clean river sand (7:1, v/v). The properties of the soil measured were as follows: pH 5.81, 1.84 g/kg total nitrogen, 10.62 mg/kg Olsen-P, 25.65 mg/kg available K, 25.4% water moisture capacity, and 8.4 g/kg organic matter content. The U content was consistent with its natural background level (approximately 0.52 mg/kg). Following this, each pot received an autoclaved mixture of 8.0 kg, along with 0.1 g of $(NH_4)_2SO_4$ and 0.05 g of $KH_2PO_4$ during the seeding process and the soil moisture was adjusted to field capacity. A preliminary dose-response experiment was conducted using the same soil and *S. halepense* under a gradient of U concentrations (0, 25, 50, 75, and

100 mg/kg as $UO_2(CH_3COO)_2 \cdot H_2O$) to select a U level that would induce clear physiological stress without acute lethality and approximate field contamination near mining sites. Based on the observed growth inhibition and oxidative stress markers, a concentration of 75 mg/kg $UO_2(CH_3COO)_2 \cdot H_2O$ (equivalent to ~44 mg/kg U in soil) was selected for the main experiment. The soil used for the experiment was pre-sterilized in an autoclave for 24 h and placed in a dark environment for 14 days. After equilibration for 2 weeks, 75 mg/kg of $UO_2(CH_3COO_2) \cdot H_2O$ solution was added to the design pots. On the second day, the soil was rehydrated again to 70%–80% of field capacity. The contaminated soil was stored in a dark and moist environment, with water supplemented regularly to maintain field capacity. The U concentrations in the surface soil and subsoil were determined once a week. No significant difference was observed between the two after 4 weeks, at which point the experiment was initiated.

For plant growth, 0.3 kg of equilibrated soil was placed in the pots. *S. halepense* seeds after sterilized with 10% $H_2O_2$ for 10 min and incubated at 25 °C for 3 days were sown in pots with the density of 8 seeds per pot, 1.7 kg of the remaining equilibrated soil was added to the pots to cover the seeds. Water the soil every other day to maintain 70%–80% of field capacity, with routine management implemented. The experiment was conducted after the plants had grown for 20 weeks.

For mycoorhizal inoculation, a total of 200 g of *F. mosseae* inoculums comprising approximately 4000 spores and infected root segments from white clover was applied into each pot. Non-AMF treatment received an equivalent quantity of autoclaved (121 °C, 0.11 MPa, 24 h) inoculum and 2 mL of inoculum filtrate (filtered through a 25 μm filter) to maintain similar microbial communities, except for the AMF strain.

For shoot sampling, plants were cut at the soil surface and divided into two subsamples: one fresh subsample was immediately flash-frozen in liquid nitrogen and stored at -80 °C for subsequent analyses of enzyme activity, PAs, $H_2O_2$ content, malondialdehyde (MDA) content, and oxygen radical absorbance capacity (ORAC) assay. The other subsample was weighed to record fresh weight, deactivated at 105 °C for 30 min, and then dried to constant weight at 70 °C. After weighing to record dry weight, the dried sample was ground into a fine powder for U concentration determination.

For root sampling, the intact root ball was carefully excavated, and large clumps of soil were gently shaken off before being placed on ice. The roots were then transferred to a tray containing pre-chilled deionized water or buffer solution and gently agitated to remove adhering soil. Surface moisture was blotted dry with clean filter paper. Representative fresh fine roots were excised, immediately flash-frozen in liquid nitrogen, and stored at -80 °C for subsequent analyses, including PAs content, enzyme activity, $H_2O_2$ content, MDA content, and ORAC assay. U content in roots was determined according to the method used for aboveground plant parts.

### High-performance liquid chromatography (HPLC) analysis of PAs

HPLC analysis was carried out using a HPLC System (Waters Alliance e2695) equipped with a 2489 UV-Vis Detector. Separation was accomplished using a Symmetry $C_{18}$ column (Waters). The analytical reagents were purchased from Sigma-Aldrich.

The separation and determination of PAs was assayed according to Franchin et al. with appropriate modifications [30]. 0.1 g of leaves or roots powder was weighed, and 1 mL of extraction solution (formic acid: methanol: water = 4:1:15, v/v/v) was added. After thorough mixing, the mixture was centrifuged at 22,000 g and 10 °C for 5 min, and the supernatant was collected. The extraction was repeated 3 times. The combined supernatants were concentrated using a vacuum concentrator. After concentration, 500 μL of trichloroacetic acid (6%, v/v) was added to fully dissolve the residue. Then, 400 μL of the supernatant was taken, and 400 μL of dansyl chloride solution (5 mg/mL) and 400 μL of saturated sodium carbonate solution were added sequentially. The mixture was incubated overnight at room temperature. After completion of the reaction, 750 μL of toluene was added, and the upper toluene layer was collected. The extraction with toluene was repeated twice, and the combined toluene layers were concentrated in a vacuum concentrator. The dried residue was dissolved in 2 mL of acetonitrile and filtered through a 0.22 μm membrane before injection.

Chromatographic separation was carried out on a Symmetry $C_{18}$ column (4.6 mm × 250 mm × 5 μm) with a column temperature of 25 °C. The flow rate was 0.7 mL/min, and the injection volume was 20 μL. Mobile phase A was aqueous solution, and mobile phase B was acetonitrile. The detection wavelength was set at 230 nm. The gradient elution program was as follows: 55% to 5% A from 0 to 15 min; 5% to 0% A from 15 to 17 min; 0% to 30% A from 17 to 30 min; and 30% to 55% A from 30 to 40 min.

The Empower workstation was used to compare and analyze the results of sample and standard solutions. Combined with the calibration curves of standard substances, qualitative and quantitative analyses of PA compounds were performed.

### Arginine decarboxylase (ADC) activity assay

ADC activity was determined according to the procedure of Xu et al. [31] with some modifications. Plant tissues (1.5 g fresh weight, FW) were homogenized in 50 mM phosphate buffer (pH 6.3) supplemented with 0.1 mM

phenylmethylsulfonyl fluoride (PMSF), 5 mM dithiothreitol (DTT), 40 μM pyridoxal phosphate (PLP), 5 mM ethylenediaminetetraacetic acid (EDTA), 40 μM polyvinylpyrrolidone (PVP) and 20 mM ascorbic acid. The homogenate was centrifuged at 15,000×g for 30 min to obtain the crude enzyme extract.

The enzymatic reaction was conducted in a total volume of 1.5 mL, comprised 0.3 mL of the enzyme extract, 0.2 mL of 25 mM L-arginine and 1 mL of assay buffer [100 mM Tris–HCl (pH 8.5), 5 mM DTT, 5 mM EDTA, 40 μM PLP]. After incubation at 37 °C for 60 min, the mixture was centrifuged at 3000×g for 10 min. A 0.5 mL sample of the supernatant was mixed with 1 mL of 2 mM NaOH, and 10 μL of benzoyl chloride was added with constant stirring for 20 s. After reacting at 25 °C for 60 min, 2 mL of saturated NaCl and 2 mL of ether were added, and the mixture was thoroughly vortexed before centrifugation at 1500×g for 5 min. A 1 mL fraction of the ether layer was collected and evaporated at 50 °C. The residue was solubilized in 0.5 mL of methanol, and its absorbance at 254 nm was measured using a HPLC system (Agilent, 1100). Enzyme activity was calculated based on an agmatine standard curve and is expressed as nmol of agmatine per minute per gram of FW.

#### Ornithine decarboxylase (ODC) activity assay

Plant tissues (1.5 g FW) were homogenized in 50 mM phosphate buffer (pH 6.8) supplemented with 0.1 mM PMSF, 5 mM DTT, 40 μM PLP, 5 mM EDTA, 40 μM PVP and 20 mM ascorbic acid. The homogenate was centrifuged at 15,000×g for 30 min to obtain the crude enzyme extract.

The enzymatic reaction was conducted in a total volume of 1.5 mL, comprised 0.3 mL of the extract, 0.2 mL of 25 mM L-ornithine and 1 mL of assay buffer [100 mM Tris–HCl (pH 7.5), 5 mM DTT, 5 mM EDTA, 40 μM PLP]. Following incubation at 37 °C for 60 min, the mixture was centrifuged at 3000×g for 10 min. A 0.5 mL sample of the supernatant was mixed with 1 mL of 2 mM NaOH, and 10 μL of benzoyl chloride was added with constant stirring for 20 s. After reacting at 25 °C for 60 min, 2 mL of saturated NaCl and 2 mL of ether were added, and the mixture was thoroughly vortexed before centrifugation at 1500×g for 5 min. A 1 mL fraction of the ether layer was collected and evaporated at 50 °C. The residue was solubilized in 0.5 mL of methanol, and its absorbance at 254 nm was measured using a HPLC system (Agilent, 1100). Enzyme activity was calculated based on an agmatine standard curve and is expressed as nmol of putrescine per minute per gram of FW.

#### Diamine oxidase (DAO) and polyamine oxidase (PAO) activities assay

DAO and PAO activities were determined spectrophotometrically with minor modifications by measuring the generation of $\Delta^1$-pyrroline, a product of the oxidation of PAs, as described by Quinet et al. [32]. Plant tissues (2 g FW) were homogenized in triplicate at 4 °C in 100 mM potassium phosphate buffer (pH 7.0) supplemented with 5 mM dithiothreitol. The homogenate was centrifuged at 15,000×g for 20 min at 4 °C, and the resulting residue was sequentially extracted twice for 10 min with 100 mM potassium phosphate buffer (pH 7.0) containing 1 mM NaCl.

The enzymatic reaction was conducted in a total volume of 1.0 ml, 450 μl of the extracted enzyme solution was mixed with 50 μl of catalase (50 U, Sigma-Aldrich) and 250 μl of 0.1% 2-aminobenzaldehyde. The reaction was initiated by adding two different substrate-buffer combinations: for DAO, 250 μl of 10 mM Put in 50 mM potassium phosphate buffer (pH 7.5) was used; for PAO, 250 μl of 10 mM Spd in 50 mM potassium phosphate buffer (pH 6.0) was employed. The reaction was incubated at 30 °C for 3 h and then terminated by adding 1.0 ml of 10% (v/v) perchloric acid (PCA). After centrifugation at 5000×g for 15 min, the formation of $\Delta^1$-pyrroline was measured by recording the absorbance at 430 nm using a HPLC system (Agilent, 1100). Enzyme activity was calculated as nmol $\Delta^1$-pyrroline per minute per gram of FW.

#### Oxygen radical absorbance capacity assay

ORAC assay was evaluated based on the method described by Cao et al. [33]. with minor adaptations. Briefly, 37.5 μL of methanol extract was combined with 225 μL of freshly prepared fluorescein solution (4 μM) and incubated at 37°C for 30 minutes. Subsequently, 37.5 μL of freshly prepared 2,2'-azobis(2-methylpropionamidine) dihydro-chloride (AAPH) was introduced to initiate the reaction. Fluorescence was monitored for 120 min using a Tecan Infinite 200 Pro M Nano$^+$ plate reader (Männedorf, Switzerland) at excitation and emission wavelengths of 485 nm and 528 nm, respectively. A Trolox standard curve was constructed using serial dilutions, and the results were quantified relative to this curve. The antioxidant capacity is expressed as micromoles of Trolox equivalents (TE) per gram of FW (μmol TE/g FW).

#### Malondialdehyde assay

MDA was determined according to Taïbi et al. [34]. Plant tissues (0.5 g FW) were homogenized in 5% (w/v) trichloroacetic acid (TCA). A 1 mL aliquot of the resulting supernatant was mixed with 4 mL of a solution containing 0.5% (w/v) thiobarbituric acid (TBA) in 20% (w/v) TCA. The mixture was heated at 95 °C for 30 min, rapidly

cooled, and then centrifuged at 10,000×g for 10 min at 4 °C.

The absorbance of the supernatant was measured at 532 nm using a multi-mode microplate reader (Tecan, Spark), with nonspecific absorption corrected by subtracting the absorbance value at 600 nm. Lipid peroxidation products were quantified as TBA-reactive substances, and MDA content was calculated using its extinction coefficient 155/(mMcm). Results were expressed as μmol MDA per gram of FW.

#### Estimation of hydrogen peroxide content

$H_2O_2$ levels were determined described by Horváth et al. [35]. Plant tissues (0.2 g FW) were homogenized in a pre-chilled mortar with 2 mL of cold acetone. The homogenate was then centrifuged at 10,000×g for 15 min at 4 °C. Subsequently, 0.5 mL of the resulting supernatant was mixed with 50 μL of titanium tetrachloride ($TiCl_4$, 20% w/v) and 0.1 mL of concentrated ammonium hydroxide. The mixture was vortexed thoroughly and centrifuged at 3000×g for 5 min at 4 °C. The pellet was washed four times with 2 mL of cold acetone, with centrifugation after each wash. The final washed precipitate was dissolved in 3 mL of 2 M sulfuric acid and the absorbance of the solution was measured at 415 nm using a spectrophotometer (Thermo Fisher, Evolution 201). The $H_2O_2$ concentration was quantified from a standard curve prepared with known concentrations of $H_2O_2$ subjected to the same procedure. Results were expressed as μmol $H_2O_2$ per gram of FW.

#### Determination of the U concentration

Plant tissues (2.0–3.0 g FW) were dried, ground and sieved through an 80-mesh sieve. A 0.500 g subsample of the dried material was placed into a digestion vessel of a microwave digestion system (CEM, Mars6). Then, 4 mL of $HNO_3$ and 2 mL of $H_2O_2$ were added (at a ratio of 2:1, v/v). After standing for 1 h, microwave digestion was performed with a three-step temperature-controlled program. The maximum microwave power was set to 1600 W. In Step 1, the temperature was ramped to 120 °C over 10 min and held for 3 min. In Step 2, the temperature was ramped to 160 °C over 5 min and held for 6 min. In Step 3, the temperature was ramped to 180 °C over 5 min and held for 15 min. Following digestion, the samples were subjected to acid evaporation on a matching hot plate at 140 °C, then diluted with 2% (v/v) $HNO_3$ to 25 mL. An aliquot of this digest was further diluted 20-fold wih 2% $HNO_3$ prior to ICP-MS analysis to bring the U concentration within the calibrated range.

U concentrations was determined using ICP-MS (Agilent, 7900) on a dry weight (DW) basis. ICP-MS operating conditions: RF power 1500 W, plasma gas flow 15 L·min$^{-1}$, auxiliary gas flow 0.15 L·min$^{-1}$, nebulizer gas flow 0.95 L·min$^{-1}$, sampling depth 8 mm, peristaltic pump speed 0.1 r·s$^{-1}$, peak hopping mode, 50 sweeps, 3 replicates, and KED mode with He flow 3.5 mL·min$^{-1}$. To compensate for matrix effects and signal drift, a 20 μg/L rhenium internal standard was introduced online via a T-junction before the nebulizer. External calibration was performed using U standards prepared in % $HNO_3$ at concentrations of 0, 20, 50, 100, 200, and 300 μg/L. A reagent blank was analyzed for background correction. The internal standard recovery was monitored throughout the analytical sequence and remained between 8% and 12% for all samples.

#### Data analysis

Data were analyzed using the software SAS System. The data underwent a combined ANOVA and the means that showed significant differences were distinguished at $P < 0.05$ by the least significant difference test. All figures were generated using GraphPad Prism.

## Results

#### Changes in PAs concentration

The contents of free PAs (Put, Spd and Spm) in roots and leaves were significantly influenced by U contamination and *F. mosseae* inoculation. U contamination significantly increased the accumulation of free PAs in roots and leaves of *S. halepense* (Fig. 1a-c). In NUCS, inoculation did not significantly alter free Put content in either roots or leaves (Fig. 1a). Under U contamination, however, inoculation led to a significant reduction in Put levels in both organs compared to non-inoculated plants, decreasing to 0.70-fold in roots and 0.77-fold in leaves (Fig. 1a). In contrast, free Spd responded differently. Inoculation increased its content in roots under both soil conditions, among them, in U-contaminated soil, inoculation increased the Spd content to 1.58-fold. While in leaves, a significant promoting effect was observed only under U stress (1.71-fold) (Fig. 1b). For free Spm, inoculation consistently enhanced its accumulation in both roots and leaves, regardless of U contamination. Specifically in UCS, inoculation with *F. mosseae* increased the Spm content to 1.31-fold in roots and 1.49-fold in leaves. (Fig. 1c).

Overall, U contamination generally increased PAs contents. Inoculation with *F. mosseae* further amplified this response for Spd and Spm under U stress, while it significantly suppressed Put accumulation in both roots and leaves under contaminated conditions.

The contents of PS-conjugated PAs (Put, Spd, and Spm) in roots and leaves were significantly influenced by U contamination and *F. mosseae* inoculation. U contamination itself promoted their accumulation, while inoculation further differentially modulated each PA. Inoculation consistently enhanced PS-conjugated Spd

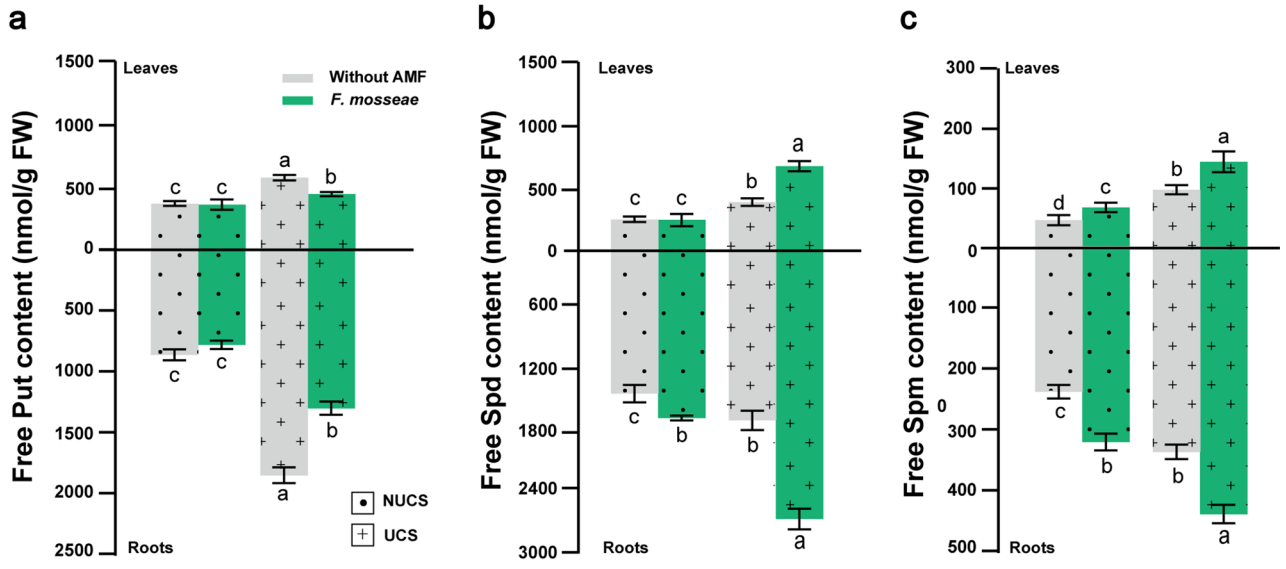



**Fig. 1** The free PA (Put, Spd and Spm) content in roots or leaves of *S. halepense* inoculated without AMF or with *F. mosseae* in non-U and U contamination soils. The different letters, separately for roots or leaves, indicate significant differences at $P \leq 0.05$ level, each value represents the mean ± SD of three replicates

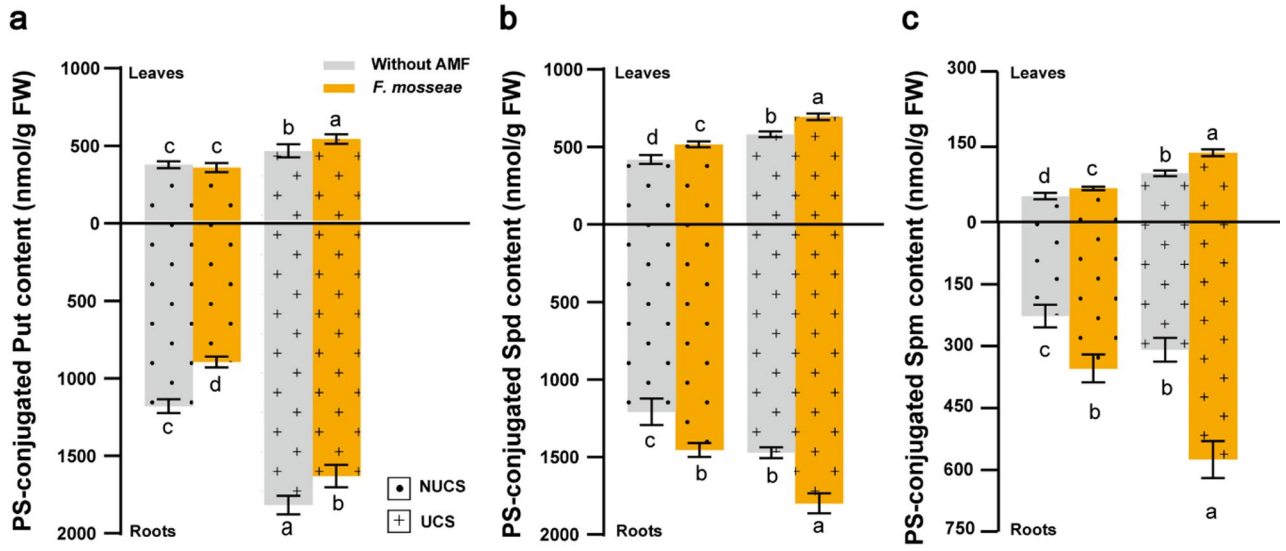



**Fig. 2** The PS-conjugared PA (Put, Spd and Spm) content in roots or leaves of *S. halepense* inoculated without AMF or with *F. mosseae* in non-U and U contamination soils. The different letters, separately for roots or leaves, indicate significant differences at $P \leq 0.05$ level, each value represents the mean ± SD of three replicates

and Spm across all conditions: under non-contaminated soil, PS-conjugated Spd increased 1.20-fold (roots) and 1.24-fold (leaves) (Fig. 2b), and PS-conjugated Spm increased 1.56-fold (roots) and 1.31-fold (leaves) (Fig. 2c); under U contamination, PS-conjugated Spd increased 1.22-fold (roots) and 1.19-fold (leaves) (Fig. 2b), and PS-conjugated Spm increased 1.86-fold (roots) and 1.43-fold (leaves) (Fig. 2c). However, the effect of *F. mosseae* inoculation on PS-conjugated Put content followed a different pattern. Inoculation reduced root PS-conjugated Put to 0.76-fold (non-contaminated) and 0.90-fold (U-contaminated) (Fig. 2a). In leaves, it had no significant effect in non-contaminated soil but increased PS-conjugated Put content 1.17-fold under U contamination (Fig. 2a).

The contents of PIS-conjugated PAs (Put, Spd, and Spm) in roots and leaves were significantly influenced by both U contamination and *F. mosseae* inoculation (Fig. 3). U contamination generally promoted the accumulation of PIS-conjugated PAs in both roots and leaves. Nevertheless, *F. mosseae* inoculation differentially regulated the content of each conjugated PA. In non-contaminated

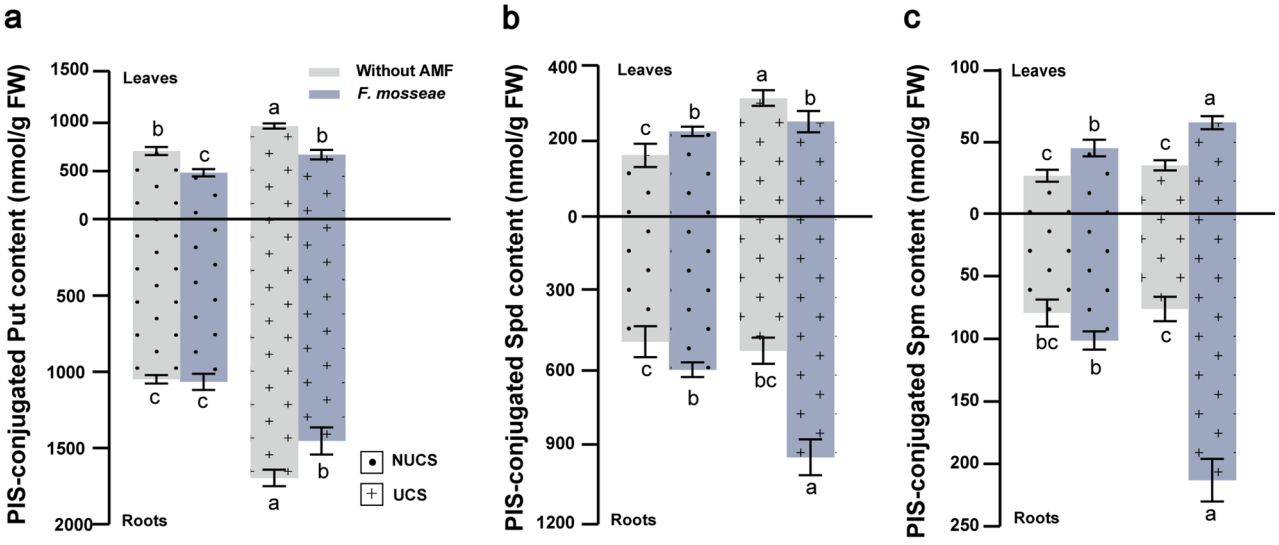



**Fig. 3** The PIS-conjugared PA (Put, Spd and Spm) content in roots or leaves of *S. halepense* inoculated without AMF or with *F. mosseae* in non-U and U contamination soils. The different letters, separately for roots or leaves, indicate significant differences at $P \leq 0.05$ level, each value represents the mean ± SD of three replicates

**Table 1** The total PA (Put, Spd and Spm) contents in roots of *S. halepense* inoculated without AMF or with *F. mosseae* in non-U and U contamination soils

| Soil | AMF | Total polyamine content (nmol/g FW) | | | |
|---|---|---|---|---|---|
| | | Put | Spd | Spm | (Spd + Spm)/Put |
| Without U | Non-AMF | 3034.17 ± 95.99 c | 3348.50 ± 78.94 c | 616.50 ± 21.00 c | 1.31 |
| | *F. mosseae* | 2681.00 ± 11.62 d | 3669.69 ± 41.68 b | 764.72 ± 36.72 b | 1.65 |
| With U | Non-AMF | 5288.98 ± 105.05 a | 3372.98 ± 129.30 c | 628.20 ± 29.89 c | 0.76 |
| | *F. mosseae* | 4297.72 ± 111.30 b | 5316.64 ± 160.86 a | 1210.29 ± 55.89 a | 1.51 |
| LSD | | 170.43 | 211.69 | 71.73 | |
| *Analysis of variance*: | | | | | |
| Mycorrhizal | | ** | ** | ** | |
| U | | ** | ** | ** | |
| Mycorrhizal ╳ U | | ** | ** | ** | |

Total contents of Put, Spd, and Spm were calculated by the summation offree PAs, PS-conjugated PAs, and PIS-bound PAs, respectively. The different letters indicate significant differences at $P \leq 0.05$ level, each value represents the mean ± SD of three replicates. ** $P < 0.01$

soil, inoculation elevated Spd (roots: 1.22-fold; leaves: 1.39-fold) and Spm (roots: 1.28-fold; leaves: 1.72-fold) (Fig. 3b-c), whereas Put was only significantly reduced in leaves (0.68-fold) (Fig. 3a). Under U contamination, inoculation with *F. mosseae* differentially regulated the contents of PIS-conjugated PAs in a PA- and organ-specific manner. PIS-conjugated Put was reduced in both leaves (0.69-fold) and roots (0.86-fold) (Fig. 3a). PIS-conjugated Spd increased markedly in roots (1.79-fold) but decreased in leaves (0.80-fold) (Fig. 3b). PIS-conjugated Spm was strongly enhanced in both organs, especially in roots (2.80-fold) and leaves (1.88-fold) (Fig. 3c).

The total PA contents in roots of *S. halepense* were significantly influenced by U contamination and inoculation with *F. mosseae* (Table 1). U contamination alone (without inoculation) dramatically increased the total Put content by 1.74-fold compared to the non-contaminated control. In contrast, under U contamination, *F. mosseae* inoculation reduced the total Put content by 0.81-fold relative to the non-inoculated U-stressed plants. The total Spd and Spm contents responded differently. In U-contaminated soil, inoculation with *F. mosseae* increased total Spd by 1.58-fold and total Spm by 1.93-fold compared to the non-inoculated U-stressed condition. The (Spd + Spm)/Put ratio, an indicator of PA homeostasis, was severely reduced by U contamination in non-inoculated plants to 0.58-fold of the non-contaminated control value. However, inoculation under U stress restored this ratio to 1.51, which was 1.99-fold higher than that in the non-inoculated U-stressed plants and even 1.15-fold higher than in the non-contaminated, non-inoculated control.

The total PA contents in leaves of *S. halepense* were significantly influenced by U contamination and inoculation with *F. mosseae* (Table 2). U contamination markedly increased the total Put content. In non-inoculated

**Table 2** The total PA (Put, Spd and Spm) content in leaves of *S. halepense* inoculated without AMF or with *F. mosseae* in non-U and U contamination soils

| Soil | AMF | Total polyamine content (nmol/g FW) | | | |
|---|---|---|---|---|---|
| | | Put | Spd | Spm | (Spd + Spm)/Put |
| Without U | Non-AMF | 1394.77 ± 44.94 c | 1282.23 ± 48.57 b | 127.14 ± 4.55 c | 1.01 |
| | *F. mosseae* | 1254.36 ± 76.07 d | 1387.49 ± 60.38 a | 135.09 ± 3.69 c | 1.21 |
| With U | Non-AMF | 1941.47 ± 39.07 a | 930.29 ± 65.13 c | 250.77 ± 17.10 b | 0.61 |
| | *F. mosseae* | 1604.08 ± 58.91 b | 1012.74 ± 28.35 c | 320.90 ± 15.76 a | 0.83 |
| LSD | | 106.52 | 98.96 | 22.59 | |
| *Analysis of variance*: | | | | | |
| Mycorrhiza | | ** | * | ** | |
| U | | ** | ** | ** | |
| Mycorrhiza ╳ U | | * | NS | ** | |

Total contents of Put, Spd, and Spm were calculated by the summation offree PAs, PS-conjugated PAs, and PIS-bound PAs, respectively. The different letters indicate significant differences at $P \leq 0.05$ level, each value represents the mean ± SD of three replicates. ** $P < 0.01$; NS: no significance

**Table 3** The activities of DAO, PAO, ADC and ODC in roots of *S. halepense* inoculated without AMF or with *F. mosseae* in non-U and U contamination soils

| Soil | AMF | Polyamine metabolic enzymes | | | |
|---|---|---|---|---|---|
| | | Diamine oxidase (DAO) [nmol $\Delta^1$-pyrroline/min/g FW] | Polyamine oxidase (PAO) [nmol $\Delta^1$-pyrroline/min/g FW] | Arginine decarboxylase (ADC) [nmol Agm/ min/g FW] | Ornithine decarboxylase (ODC) [nmol Put/min/g FW] |
| Without U | Non-AMF | 18.83 ± 1.75 c | 11.59 ± 1.16 c | 1.55 ± 0.17 c | 0.92 ± 0.05 b |
| | *F. mosseae* | 20.78 ± 1.71 c | 12.31 ± 0.60 c | 1.75 ± 0.14 c | 1.13 ± 0.15 b |
| With U | Non-AMF | 25.66 ± 1.70 b | 15.15 ± 0.52 b | 2.71 ± 0.10 b | 1.14 ± 0.08 b |
| | *F. mosseae* | 46.58 ± 1.92 a | 27.37 ± 1.36 a | 6.79 ± 0.59 a | 3.89 ± 0.30 a |
| LSD | | 3.34 | 1.84 | 0.83 | 0.33 |
| *Analysis of variance*: | | | | | |
| Mycorrhizal | | ** | ** | ** | ** |
| U | | ** | ** | ** | ** |
| Mycorrhizal ╳ U | | ** | ** | ** | ** |

The different letters indicate significant differences at $P \leq 0.05$ level, each value represents the mean ± SD of three replicates. **, $P < 0.01$

leaves, U stress raised Put levels by 1.39-fold. Inoculation with *F. mosseae* under U contamination resulted in a Put content that was 0.83-fold lower than in the non-inoculated control. In contrast, the total Spd content in leaves decreased to about 0.73-fold under U stress. Inoculation with *F. mosseae* under U contamination increased the Spd content to approximately 1.09-fold compared to the non-inoculated control. However, the total Spm content responded positively to U stress. U contamination increased Spm content by 1.97-fold compared to the non-contaminated control. When plants were inoculated, the Spm content increased to 1.27-fold of that in the non-inoculated control. The (Spd + Spm)/Put ratio, an indicator of PA homeostasis, was substantially reduced by U contamination. In non-inoculated leaves, the ratio dropped to 0.60-fold of the non-contaminated control value. When inoculated, the ratio increased to 1.36-fold of that in the non-inoculated control.

### Changes in PA metabolic enzyme activities

The activities of key enzymes involved in PA metabolism in sorghum roots were significantly influenced by U contamination and inoculation with *F. mosseae* (Table 3). Analysis of variance indicated that the main effects of mycorrhizal inoculation, U contamination, and their interaction were all highly significant ($P < 0.01$) for all four enzymes assayed.

U contamination increased the activities of DAO, PAO, ADC, and ODC (Table 3). However, inoculation with *F. mosseae* under U stress further and significantly enhanced this increase for all enzymes. Specifically, inoculation with AMF increased the activities of DAO, PAO, ADC, and ODC by 1.82-, 1.81-, 2.51-, and 3.41-fold, respectively, compared to non-AMF plants in contaminated soil (Table 3).

The activities of key PA metabolic enzymes in sorghum leaves were significantly modulated by both U contamination and inoculation with *F. mosseae*, though the response patterns differed from those in roots (Table 4). Analysis of variance indicated that mycorrhizal inoculation, U contamination, and their interaction all exerted

**Table 4** The activities of DAO, PAO, ADC and ODC in leaves of *S. halepense* inoculated without AMF or with *F. mosseae* in non-U and U contamination soils

| Soil | AMF | Polyamine metabolic enzymes | | | |
|---|---|---|---|---|---|
| | | Diamine oxidase (DAO) [nmol $\Delta^1$-pyrroline/min/g FW] | Polyamine oxidase (PAO) [nmol $\Delta^1$-pyrroline/min/g FW] | Arginine decarboxylase (ADC) [nmol Agm /h/g FW] | Ornithine decarboxylase (ODC) [nmol Put /h/g FW] |
| Without U | Non-AMF | 7.40 ± 0.29 c | 2.37 ± 0.24 c | 0.82 ± 0.05 b | 0.37 ± 0.02 b |
| | *F. mosseae* | 5.81 ± 0.92 d | 3.44 ± 0.17 b | 0.90 ± 0.06 b | 0.40 ± 0.02 b |
| With U | Non-AMF | 8.94 ± 0.39 b | 3.76 ± 0.36 b | 1.09 ± 0.25 b | 0.98 ± 0.06 a |
| | *F. mosseae* | 16.47 ± 0.93 a | 6.25 ± 0.13 a | 2.76 ± 0.19 a | 1.03 ± 0.07 a |
| LSD | | 1.35 | 0.46 | 0.30 | 0.10 |
| *Analysis of variance*: | | | | | |
| Mycorrhizal | | ** | ** | ** | NS |
| U | | ** | ** | ** | ** |
| Mycorrhizal ╳ U | | ** | ** | ** | NS |

The different letters indicate significant differences at $P \leq 0.05$ level, each value represents the mean ± SD of three replicates. ** $P < 0.01$; NS: no significance

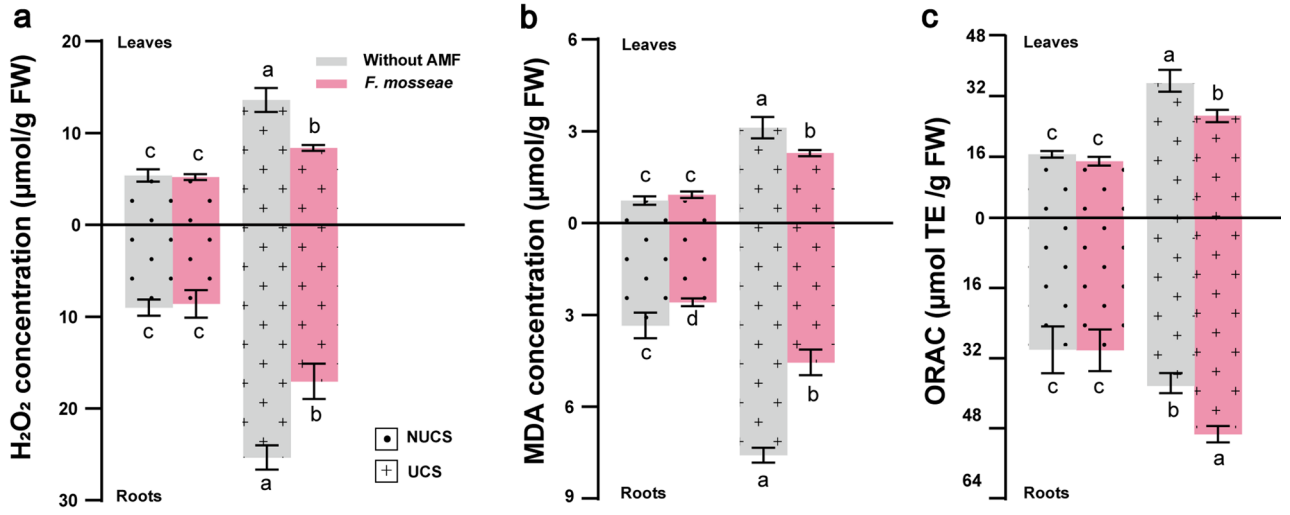



**Fig. 4** The $H_2O_2$ (**a**) and MDA content (**b**), oxygen radical absorbance capacity (**c**) in roots or leaves of *S. halepense* inoculated without AMF or with *F. mosseae* in non-U and U contamination soils. The different letters, separately for roots or leaves, indicate significant differences at $P \leq 0.05$ level, each value represents the mean ± SD of three replicates

highly significant effects ($P < 0.01$) on DAO, PAO, and ADC activities. In contrast, ODC activity was significantly affected only by U contamination, with no significant main effect of inoculation or interaction.

U contamination significantly enhanced the activities of all four PA-metabolizing enzymes with highly significant effects. Under U-contaminated conditions, inoculation with *F. mosseae* exerted differential impacts: it significantly increased DAO (to 1.84-fold), PAO (to 1.66-fold), and ADC (2.53-fold) activities, however, a significant additional change was not induced in ODC activity, compared to non-AMF plants (Table 4).

### Changes in $H_2O_2$, MDA and ORAC

U contamination induced severe oxidative stress in both roots and leaves of *S. halepense*. In non-inoculated plants, U exposure significantly increased key oxidative stress markers: $H_2O_2$ concentration rose to 2.81-fold in roots and 2.53-fold in leaves compared to non-contaminated controls (Fig. 4a). Concurrently, the level of MDA, a marker of membrane lipid peroxidation, increased to 2.26-fold in roots and a pronounced 4.23-fold in leaves (Fig. 4b).

Inoculation with *F. mosseae* significantly alleviated this U-induced oxidative damage. Under U stress, AMF colonization reduced $H_2O_2$ accumulation to 0.67-fold in roots and 0.62-fold in leaves relative to non-inoculated plants (Fig. 4a). Similarly, MDA content was lowered to 0.60-fold in roots and 0.73-fold in leaves (Fig. 4b).

Analysis of the ORAC revealed that U contamination activated the plant's antioxidant defense system. In non-inoculated plants, U exposure elevated ORAC values to 1.27-fold in roots and 2.12-fold in leaves of the control levels (Fig. 4c). Interestingly, *F. mosseae* inoculation

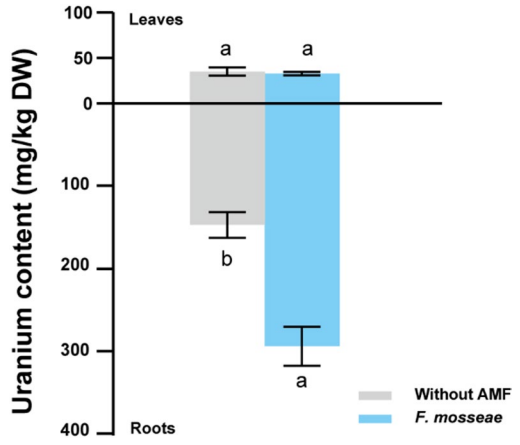



**Fig. 5** The U content in roots or leaves of *S. halepense* inoculated without AMF or with *F. mosseae* in U contamination soils. The different letters, separately for roots or leaves, indicate significant differences at $P \leq 0.05$ level, each value represents the mean ± SD of three replicates

exerted differential regulatory effects in roots and leaves, it enhanced the antioxidant capacity in root under U stress to 1.30-fold of the non- inoculated plants, whereas in leaves, it resulted in a reduction to 0.74-fold of the non-inoculated plants (Fig. 4c).

### U concentration

Inoculation with *F. mosseae* specifically enhanced U accumulation in the roots of *S. halepense* (Fig. 5). The root U concentration in inoculated plants (293.94 mg/kg DW) was approximately 1.99-fold higher than that in non-inoculated plants (147.35 mg/kg DW) (Fig. 5). In contrast, leaf U concentration remained low (< 50 mg/kg DW) and unaffected by inoculation, with no significant difference between treatments (Fig. 5).

## Discussion

The present study demonstrates that inoculation with the *F. mosseae* markedly alleviates U-induced oxidative stress in *S. halepense*, primarily through the modulation of PA metabolism and the enhancement of antioxidant capacity. Under U stress, AMF colonization increased the activities of ADC and ODC, thereby promoting Put synthesis. Concurrently, the activities of DAO and PAO were elevated, which facilitated the conversion of Put to Spd and Spm. These metabolic shifts resulted in a higher (Spd + Spm)/Put ratio, a key indicator of improved PA homeostasis and stress tolerance. In addition, AMF inoculation reduced the levels of MDA and $H_2O_2$ and increased the ORAC activity in the roots, while specifically enhancing the accumulation of U within the root system. These interconnected responses suggest that AMF mediates a coordinated physiological reprogramming that enhances U tolerance.

A conserved early response to heavy metal stress is the accumulation of Put, a non-specific biomarker of metal toxicity observed in Cd, copper (Cu), mercury (Hg), aluminium (Al), As, Cr, and Ni [36–41]. In our study, U stress similarly induced a significant increase in free, PS-, and PIS-conjugated Put in *S. halepense* roots and leaves, aligning with this conserved pattern. However, the metabolic fate of Put and the homeostasis of higher-order PAs (Spd and Spm) reveal a critical divergence. Under Cd, Cu, Hg, Al, As, and Cr stress, Spd and Spm levels typically remain unchanged or decline, whereas our data show that U stress consistently elevated free, PS-, and PIS-conjugated Spd and Spm in both roots and leaves (Figs. 1, 2 and 3). This divergence is further underscored by the distinct regulation of catabolic enzymes. While upregulation of biosynthetic enzymes (ADC, ODC) is a common response to metals [36–38, 42, 43], U stress uniquely induced a co-activation of both DAO and PAO (Tables 3 and 4), albeit with tissue-specific patterns: in roots, ADC was upregulated while ODC remained unchanged; in leaves, ODC was upregulated while ADC remained unchanged. This contrasts with the suppression or undetectable activity of DAO and PAO reported under Cd, Cu, Hg, and Ni stress [36, 37, 44]. This coordinated upregulation of both synthetic and catabolic branches reflects a more dynamic and finely tuned PA metabolic cycle in response to U stress. The tissue-specific activation of ADC or ODC ensures a sustained supply of Put, while the co-activation of DAO and PAO serves multiple functions: it generates $H_2O_2$ as a signaling molecule to activate downstream defense responses, enables precise regulation of the ratio between Put and higher-order PAs (Spd/Spm) to meet distinct protective and regulatory demands in roots versus leaves, and it prevents the potential toxicity associated with excessive Put accumulation, thereby maintaining metabolic homeostasis. Such distinctive PA metabolic profiles under U stress likely arise from its unique chemical and physical properties: the linear uranyl oxy-cation ($UO_2^{2+}$) differs structurally from spherical divalent cations; its radioactivity may impose persistent oxidative stress and DNA damage, preferentially mobilizing Spm as a protective molecule; and it may perturb nitrogen metabolism in ways that alter precursor availability for PA biosynthesis in a tissue-specific manner.

AMF orchestrates a sophisticated reprogramming of PA metabolism under U stress, strategically directing both overall production and the conversion of PAs into specific, functionally dedicated pools. Our data show that U stress alone elevated the levels of free, PS-conjugated, and PIS-conjugated Put in roots and leaves, supported by increased ADC and ODC activities. Crucially, inoculation with *F. mosseae* under U stress not only amplified this biosynthetic push but also strongly enhanced the activities of catabolic enzymes (DAO and PAO). This

coordinated regulation promotes the critical conversion of accumulated Put to the protective higher-order PAs, Spd and Spm. This metabolic shift is evidenced by the restoration of the (Spd + Spm)/Put ratio in AMF-inoculated plants and is physiologically significant. The positive correlation between antioxidant capacity (ORAC) and free Spd ($r$ = 0.71, $P$ < 0.01) or Spm ($r$ = 0.84, $P$ < 0.01) underscores their key role in mitigating oxidative stress, as Spd and Spm are more effective than Put in scavenging ROS and stabilizing membranes [24].

Our results demonstrate that U stress alone induced significant oxidative stress, as evidenced by increased $H_2O_2$ and MDA levels, consistent with previous studies [45]. AMF inoculation decreased $H_2O_2$ and MDA while increasing root ORAC (Fig. 4a-c). This indicates that AMF exerts fine-tuned regulation over $H_2O_2$ homeostasis, potentially transforming it from a toxic molecule into a beneficial signal. We hypothesize this is achieved through: (i) source regulation: AMF enhances PA catabolic enzymes (DAO and PAO) under U stress, anchoring $H_2O_2$ production within a beneficial metabolic pathway (Put→Spd/Spm conversion), thus priming it for signaling roles [23]. (ii) spatiotemporal precision control: DAO/PAO activity and $H_2O_2$ production may be localized to specific compartments (e.g., periarbuscular interface), where low-dose $H_2O_2$ can activate defense or symbiotic signaling without causing widespread damage [16]. (iii) enhanced scavenging capacity: increased root ORAC provides a buffer to quench excess $H_2O_2$, keeping its concentration below damaging thresholds [21]. (iv) signal integration: within AMF symbiosis, $H_2O_2$ likely engages in crosstalk with other symbiotic and stress signals (e.g., calcium, nitric oxide) [46], reprogramming the host's response network to favor adaptation.

This fine-tuned regulation is further evidenced by an organ-level division of labor, thus, the enhanced root ORAC but decreased leaf ORAC under U stress with AMF. Roots enhance antioxidant capacity to manage the localized demands of symbiosis interface construction and U immobilization, aligning with increases in cell wall-bound PAs (PIS-Spd/Spm). The successful immobilization of U in roots reduces translocation to shoots, which may allow leaves to downregulate antioxidant investment as a metabolic optimization, reallocating resources to growth and photosynthesis. This exemplifies a coordinated redox recalibration between organs to facilitate a beneficial partnership with AMF.

The efficacy of this AMF-mediated reprogramming is critically influenced by the environmental context, particularly soil pH, which dictates U bioavailability. Soil pH regulates U's environmental behavior through morphological transformation, adsorption-precipitation, and ion interaction [5]. Our experimental pH of 5.81 simulates acidic conditions common near U mining sites, where U (VI) exists predominantly as the soluble and bioavailable $UO_2^{2+}$ [45]. This high bioavailability under acidic conditions underscores the severity of the physiological disruption observed in non-mycorrhizal plants and, conversely, highlights the remarkable effectiveness of the AMF-induced tolerance mechanisms described above.

The coordinated physiological and biochemical responses orchestrated by AMF directly translate into an effective phytoremediation strategy. Beyond enhancing physiological tolerance, *F. mosseae* played a crucial role in modulating U distribution within the plant—a finding with direct implications for phytoremediation strategy selection. AMF inoculation significantly increased the U concentration in roots by 1.99-fold but did not affect U levels in leaves (Fig. 5). This pattern aligns with the consensus that AMF primarily facilitates U phytostabilization rather than phytoextraction [47]. The mechanisms are multifaceted: extraradical hyphae extend soil exploration [48]; U is immobilized via adsorption/chelation by fungal-secreted compounds [49]; and critically, U-rich particles are formed within intraradical fungal structures (16), providing direct evidence for fungal compartmentalization. This root sequestration blocks environmental migration, alleviates phytotoxicity, prevents food chain entry, reduces remediation costs, and ensures ecologically safer containment of U's dual risks [50].

This study elucidates key physiological aspects of AMF-enhanced U tolerance but has limitations that point to future directions. Primarily, the lack of biomass data precludes a full assessment of phytoremediation potential. Additionally, while oxidative stress was gauged via $H_2O_2$ and MDA, a fuller picture of the antioxidant system requires measuring key enzyme activities. Future research should integrate these measurements. Furthermore, structural equation modeling could be employed to quantitatively elucidate the relationships among PA metabolism, antioxidant activity, and U accumulation. Ultimately, molecular-level analyses (e.g., of gene expression in PA pathways) are needed to confirm biochemical observations and uncover regulatory mechanisms.

## Conclusions

In conclusion, this study demonstrates that inoculation with *F. mosseae* alleviated U-induced oxidative stress in *S. halepense* by modulating PA metabolism. Specifically, AMF promotes the conversion of Put to Spd and Spm, thereby maintaining a higher (Spd + Spm)/Put ratio and enhancing antioxidant capacity. Moreover, AMF increased U accumulation in roots while limiting its translocation to leaves, which may be advantageous for phytostabilization. These findings highlight the potential of AMF-assisted phytoremediation for U-contaminated soils. Future research should integrate physiological, molecular, and field-scale approaches to fully exploit

the synergistic effects of AMF and plants for sustainable environmental remediation.

**Author contributions**
Conceptualization: Y.Z. and B.L.; methodology: Y.Z., B.L. and Y.L.; software: Y.Z. and Y.L.; formal analysis: Y.Z.; investigation: Q.W.; resources: E.F.A.A.; data curation: A.H.; writing—original draft preparation: Y.Z. and Y.L.; writing—review and editing: R.H.; supervision: E.F.A.A.; project administration: R.H.; funding acquisition: R.H. All authors have read and agreed to the published version of the manuscript.

**Funding**
This work is financed by the Grants of Jingmen Science and Technology Bureau (2023YFZD014), the Opening Project of Hubei Engineering Research Center for Specialty Flowers Biological Breeding (2022ZD003), and the Fund for the Doctoral Program of Jingchu University of Technology (YY202201), the Campus level scientific research project of Jingchu University of Technology (ZD202316). The authors would like to extend their sincere appreciation to Ongoing Research Funding program (ORF-2026-356), King Saud University, Riyadh, Saudi Arabia.

**Data availability**
No datasets were generated or analysed during the current study.

## Declarations

**Ethics approval and Consent to participate**
Not applicable.

**Consent for publication**
Not applicable.

**Competing interests**
The authors declare no competing interests.

**Author details**
[1]College of Food and Biology, Jingchu University of Technology, Jingmen 448000, Hubei, China
[2]Jiangxi Academy of Forestry, Nanchang 330100, Jiangxi, China
[3]College of Horticulture and Gardening, Yangtze University, Jingzhou 434025, Hubei, China
[4]Department of Botany and Microbiology, College of Science, King Saud University, P.O. Box. 2455, 11451 Riyadh, Saudi Arabia
[5]Department of Plant Production, College of Food and Agricultural Sciences, King Saud University, P.O. Box. 2460, 11451 Riyadh, Saudi Arabia

Received: 2 November 2025 / Accepted: 6 May 2026
Published online: 24 May 2026

**References**

1. Boteva S, Radeva G, Traykov I, Kenarova A. Effects of long-term radionuclide and heavy metal contamination on the activity of microbial communities, inhabiting uranium mining impacted soils. Environ Sci Pollut Res Int. 2016;23(6):5644–53. https://doi.org/10.1007/s11356-015-5788-5.
2. Chen H, Sheng Y, Wang S, Chen Y, Qiao Z, Guo H, et al. Uranium contamination mediating soil and ore microbial community assembly at four mining sites, South China. Front Microbiol. 2025;16:1553072. https://doi.org/10.3389/fmicb.2025.1553072.
3. Alsabbagh AH, Abuqudaira TM. Phytoremediation of jordanian uranium-rich soil using sunflower. Water Air Soil Pollut. 2017;228(6):219. https://doi.org/10.1007/s11270-017-3396-3.
4. Tewari R, Horemans N, Nauts R, Wannijn J, Van Hees M, Vandenhove H. Uranium exposure induces nitric oxide and hydrogen peroxide generation in *Arabidopsis thaliana*. Environ Exp Bot. 2015;120:55–64. https://doi.org/10.1016/j.envexpbot.2015.08.004.
5. Cui Q, Zhang Z, Beiyuan J, Cui Y, Chen L, Chen H, et al. A critical review of uranium in the soil-plant system: distribution, bioavailability, toxicity, and bioremediation strategies. Crit Rev Environ Sci Technol. 2023;53(3):340–65. https://doi.org/10.1080/10643389.2022.2054246.
6. Stürmer SL, Bever JD, Morton JB. Biogeography of arbuscular mycorrhizal fungi (*Glomeromycota*): a phylogenetic perspective on species distribution patterns. Mycorrhiza. 2018;28(7):587–603. https://doi.org/10.1007/s00572-018-0864-6.
7. Wahab A, Muhammad M, Munir A, Abdi G, Zaman W, Ayaz A, et al. Role of arbuscular mycorrhizal fungi in regulating growth, enhancing productivity, and potentially influencing ecosystems under abiotic and biotic stresses. Plants. 2023;12(17):3102. https://doi.org/10.3390/plants12173102.
8. Ferrol N, Tamayo E, Vargas P. The heavy metal paradox in arbuscular mycorrhizas: from mechanisms to biotechnological applications. J Exp Bot. 2016;67(22):6253–65. https://doi.org/10.1093/jxb/erw403.
9. Göhre V, Paszkowski U. Contribution of the arbuscular mycorrhizal symbiosis to heavy metal phytoremediation. Planta. 2006;223(6):1115–22. https://doi.org/10.1007/s00425-006-0225-0.
10. Riaz M, Kamran M, Fang Y, Wang Q, Cao H, Yang G, et al. Arbuscular mycorrhizal fungi-induced mitigation of heavy metal phytotoxicity in metal contaminated soils: a critical review. J Hazard Mater. 2021;402:123919. https://doi.org/10.1016/j.jhazmat.2020.123919.
11. Sanjana S, Jazeel K, Janeeshma E, Nair SG, Shackira AM. Synergistic interactions of assorted ameliorating agents to enhance the potential of heavy metal phytoremediation. Stress Biol. 2024;4(1):13. https://doi.org/10.1007/s44154-024-00153-1.
12. Davies HS, Cox F, Robinson CH, Pittman JK. Radioactivity and the environment: technical approaches to understand the role of arbuscular mycorrhizal plants in radionuclide bioaccumulation. Front Plant Sci. 2015;6:580. https://doi.org/10.3389/fpls.2015.00580.
13. Chen B, Jakobsen I, Roos P, Zhu Y-G. Effects of the mycorrhizal fungus *Glomus intraradices* on uranium uptake and accumulation by *Medicago truncatula* L. from uranium-contaminated soil. Plant Soil. 2005;275(1):349–59. https://doi.org/10.1007/s11104-005-2888-x.
14. Chen BD, Zhu YG, Smith FA. Effects of arbuscular mycorrhizal inoculation on uranium and arsenic accumulation by Chinese brake fern (*Pteris vittata* L.) from a uranium mining-impacted soil. Chemosphere. 2006;62(9):1464–73. https://doi.org/10.1016/j.chemosphere.2005.06.008.
15. Ren C-G, Kong C-C, Wang S-X, Xie Z-H. Enhanced phytoremediation of uranium-contaminated soils by arbuscular mycorrhiza and rhizobium. Chemosphere. 2019;217:773–9. https://doi.org/10.1016/j.chemosphere.2018.11.085.
16. Dinsley JM, Halsey K, Venter E, Gomez-Gonzalez MA, Moore KL, Field LP, et al. Arbuscular mycorrhizal fungi influence the speciation and subcellular abundance of uranium in plant roots. Environ Sci Process Impacts. 2025;27(8):2394–409. https://doi.org/10.1039/d5em00108k.
17. Gholami M, Fakhari AR, Ghanati F. Selective regulation of nicotine and polyamines biosynthesis in tobacco cells by enantiomers of ornithine. Chirality. 2013;25(1):22–7. https://doi.org/10.1002/chir.22107.
18. Kim DW, Watanabe K, Murayama C, Izawa S, Niitsu M, Michael AJ, et al. Polyamine oxidase5 regulates arabidopsis growth through thermospermine oxidase activity. Plant physiol. 2014;165(4):1575–90. https://doi.org/10.1104/pp.114.242610.
19. Alcázar R, Altabella T, Marco F, Bortolotti C, Reymond M, Koncz C, et al. Polyamines: molecules with regulatory functions in plant abiotic stress tolerance. Planta. 2010;231(6):1237–49. https://doi.org/10.1007/s00425-010-1130-0.
20. Sobieszczuk-Nowicka E. Polyamine catabolism adds fuel to leaf senescence. Amino Acids. 2017;49(1):49–56. https://doi.org/10.1007/s00726-016-2377-y.
21. Liu J-H, Wang W, Wu H, Gong X, Moriguchi T. Polyamines function in stress tolerance: from synthesis to regulation. Front Plant Sci. 2015;6:827. https://doi.org/10.3389/fpls.2015.00827.
22. Wang W, Paschalidis K, Feng J-C, Song J, Liu J-H. Polyamine catabolism in plants: a universal process with diverse functions. Front Plant Sci. 2019;10:561. https://doi.org/10.3389/fpls.2019.00561.
23. Moschou PN, Wu J, Cona A, Tavladoraki P, Angelini R, Roubelakis-Angelakis KA. The polyamines and their catabolic products are significant players in the turnover of nitrogenous molecules in plants. J Exp Bot. 2012;63(14):5003–15. https://doi.org/10.1093/jxb/ers202.
24. Chen D, Shao Q, Yin L, Younis A, Zheng B. Polyamine function in plants: metabolism, regulation on development, and roles in abiotic stress responses. Front Plant Sci. 2019;9:1945. https://doi.org/10.3389/fpls.2018.01945.
25. Akiyama K, Matsuzaki K-i, Hayashi H. Plant sesquiterpenes induce hyphal branching in arbuscular mycorrhizal fungi. Nature. 2005;435(7043):824–7. https://doi.org/10.1038/nature03608.

26. Zhang F, Zou Y-N, Wu Q-S, Kuča K. Arbuscular mycorrhizas modulate root polyamine metabolism to enhance drought tolerance of trifoliate orange. Environ Exp Bot. 2020;171:103926. https://doi.org/10.1016/j.envexpbot.2019.103926.
27. Zou YN, Zhang F, Srivastava AK, Wu QS, Kuča K. Arbuscular mycorrhizal fungi regulate polyamine homeostasis in roots of trifoliate orange for improved adaptation to soil moisture deficit stress. Front Plant Sci. 2021;11:600792. https://doi.org/10.3389/fpls.2020.600792.
28. Chowdhary NA, Songachan LS. Boosting sustainable agriculture by arbuscular mycorrhizal fungi under abiotic stress condition. Plant Stress. 2025;17:100945. https://doi.org/10.1016/j.stress.2025.100945.
29. Mishra D, Kumar S, Mishra BN. An overview of morpho-physiological, biochemical, and molecular responses of *sorghum* towards heavy metal stress. Rev Environ Contam Toxicol. 2021;256:155–77. https://doi.org/10.1007/398_2020_61.
30. Franchin C, Fossati T, Pasquini E, Lingua G, Castiglione S, Torrigiani P, et al. High concentrations of zinc and copper induce differential polyamine responses in micropropagated white poplar (*Populus alba*). Physiol Plant. 2007;130(1):77–90. https://doi.org/10.1111/j.1399-3054.2007.00886.x.
31. Xu X, Shi G, Jia R. Changes of polyamine levels in roots of *Sagittaria sagittifolia* L. under copper stress. Environ Sci Pollut. 2012;19(7):2973–82. https://doi.org/10.1007/s11356-012-0808-1.
32. Quinet M, Ndayiragije A, Lefèvre I, Lambillotte B, Dupont-Gillain CC, Lutts S. Putrescine differently influences the effect of salt stress on polyamine metabolism and ethylene synthesis in rice cultivars differing in salt resistance. J Exp Bot. 2010;61(10):2719–33. https://doi.org/10.1093/jxb/erq118.
33. Cao G, Alessio HM, Cutler RG. Oxygen-radical absorbance capacity assay for antioxidants. Free Radical Biol Med. 1993;14(3):303–11. https://doi.org/10.1016/0891-5849(93)90027-R.
34. Taïbi K, Taïbi F, Ait Abderrahim L, Ennajah A, Belkhodja M, Mulet JM. Effect of salt stress on growth, chlorophyll content, lipid peroxidation and antioxidant defence systems in *Phaseolus vulgaris* L. S Afr J Bot. 2016;105:306–12. https://doi.org/10.1016/j.sajb.2016.03.011.
35. Horváth E, Csiszár J, Gallé Á, Poór P, Szepesi Á, Tari I. Hardening with salicylic acid induces concentration-dependent changes in abscisic acid biosynthesis of tomato under salt stress. J Plant Physiol. 2015;183:54–63. https://doi.org/10.1016/j.jplph.2015.05.010.
36. Groppa MD, Tomaro ML, Benavides MP. Polyamines and heavy metal stress: the antioxidant behavior of spermine in cadmium- and copper-treated wheat leaves. Biometals. 2007;20(2):185–95. https://doi.org/10.1007/s10534-006-9026-y.
37. Ding C, Shi G, Xu X, Yang H, Xu Y. Effect of exogenous spermidine on polyamine metabolism in water hyacinth leaves under mercury stress. Plant Growth Regul. 2010;60(1):61–7. https://doi.org/10.1007/s10725-009-9419-3.
38. Yu Y, Jin C, Sun C, Wang J, Ye Y, Lu L, et al. Elevation of arginine decarboxylase-dependent putrescine production enhances aluminum tolerance by decreasing aluminum retention in root cell walls of wheat. J Hazard Mater. 2015;299:280–8. https://doi.org/10.1016/j.jhazmat.2015.06.038.
39. Mascher R, Lippmann B, Holzinger S, Bergmann H. Arsenate toxicity: effects on oxidative stress response molecules and enzymes in red clover plants. Plant Sci. 2002;163(5):961–9. https://doi.org/10.1016/S0168-9452(02)00245-5.
40. Scoccianti V, Iacobucci M, Speranza A, Antognoni F. Over-accumulation of putrescine induced by cyclohexylamine interferes with chromium accumulation and partially restores pollen tube growth in *Actinidia deliciosa*. Plant Physiol Biochem. 2013;70:424–32. https://doi.org/10.1016/j.plaphy.2013.06.004.
41. Zhao J, Shi G, Yuan Q. Polyamines content and physiological and biochemical responses to ladder concentration of nickel stress in *Hydrocharis dubia* (Bl.) backer leaves. Biometals. 2008;21(6):665–74. https://doi.org/10.1007/s10534-008-9151-x.
42. Kumar N, Gautam A, Dubey AK, Ranjan R, Pandey A, Kumari B, et al. GABA mediated reduction of arsenite toxicity in rice seedling through modulation of fatty acids, stress responsive amino acids and polyamines biosynthesis. Ecotoxicol Environ Saf. 2019;173:15–27. https://doi.org/10.1016/j.ecoenv.2019.02.017.
43. Kang Y, Li CZ, Ullah A, Zhang Q, Yu XZ. The accumulation of abscisic acid increases the innate pool of soluble phenolics through polyamine metabolism in rice seedlings under hexavalent chromium stress. Toxics. 2024;12(8):577. https://doi.org/10.3390/toxics12080577.
44. Pietrini F, Iori V, Cheremisina A, Shevyakova NI, Radyukina N, Kuznetsov VV, et al. Evaluation of nickel tolerance in *Amaranthus paniculatus* L. plants by measuring photosynthesis, oxidative status, antioxidative response and metal-binding molecule content. Environ Sci Pollut Res Int. 2015;22(1):482–94. https://doi.org/10.1007/s11356-014-3349-y.
45. Saenen E, Horemans N, Vanhoudt N, Vandenhove H, Biermans G, Van Hees M, et al. Effects of pH on uranium uptake and oxidative stress responses induced in *Arabidopsis thaliana*. Environ Toxicol Chem. 2013;32(9):2125–33. https://doi.org/10.1002/etc.2290.
46. Anam S, Hilal B, Fariduddin Q. Polyamines and hydrogen peroxide: allies in plant resilience against abiotic stress. Chemosphere. 2024;366:143438. https://doi.org/10.1016/j.chemosphere.2024.143438.
47. Ebbs SD, Brady DJ, Kochian LV. Role of uranium speciation in the uptake and translocation of uranium by plants. J Exp Bot. 1998;49(324):1183–90. https://doi.org/10.1093/jxb/49.324.1183.
48. Umer M, Anwar N, Mubeen M, Li Y, Ali A, Alshaharni MO, et al. Roles of arbuscular mycorrhizal fungi in plant growth and disease management for sustainable agriculture. Front Microbiol. 2025;16:1616273. https://doi.org/10.3389/fmicb.2025.1616273.
49. González-Chávez MC, Carrillo-González R, Wright SF, Nichols KA. The role of glomalin, a protein produced by arbuscular mycorrhizal fungi, in sequestering potentially toxic elements. Environ Pollut. 2004;130(3):317–23. https://doi.org/10.1016/j.envpol.2004.01.004.
50. Rodriguez-Freire L, DeVore CL, El Hayek E, Berti D, Ali AS, Lezama Pacheco JS, et al. Emerging investigator series: entrapment of uranium-phosphorus nanocrystals inside root cells of *Tamarix* plants from a mine waste site. Environ Sci Process Impacts. 2021;23(1):73–85. https://doi.org/10.1039/d0em00306a.


## Publisher's note

Springer Nature remains neutral with regard to jurisdictional claims in published maps and institutional affiliations.